Hadron structure

Gunnar Bali

Universität Regensburg







October 1, 2026

Larnaca, Cyprus

The standard model of particle physics

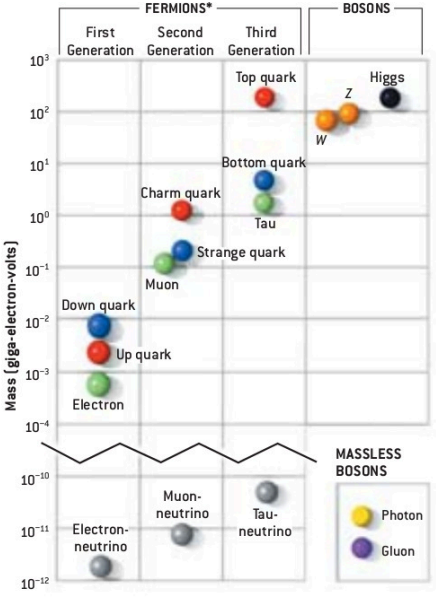

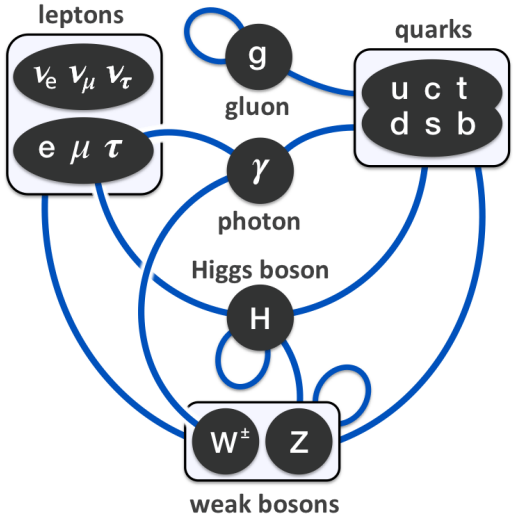

Running of Standard Model couplings with the scale

g_3: QCD coupling, g_1, g_2: Electroweak U(1), SU(2) couplings,
λ: quartic Higgs coupling, y_q: Yukawa couplings. [D Buttazzo et al, 1305.3536]

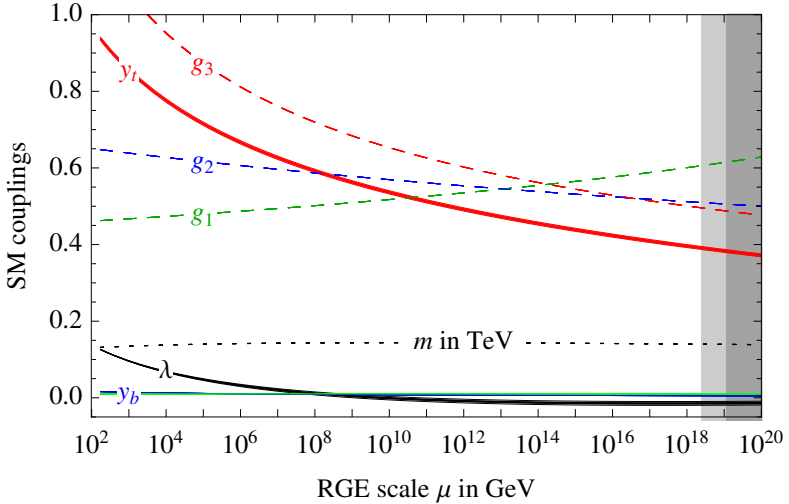

$$V(\Phi) = -m^2\Phi^\dagger\Phi + \lambda(\Phi^\dagger\Phi)^2$$
$$m_h = \sqrt{2}m, \quad v = m/\sqrt{\lambda}$$

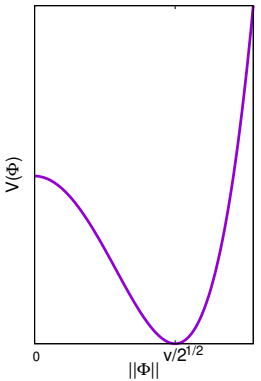

Asymptotic freedom of QCD

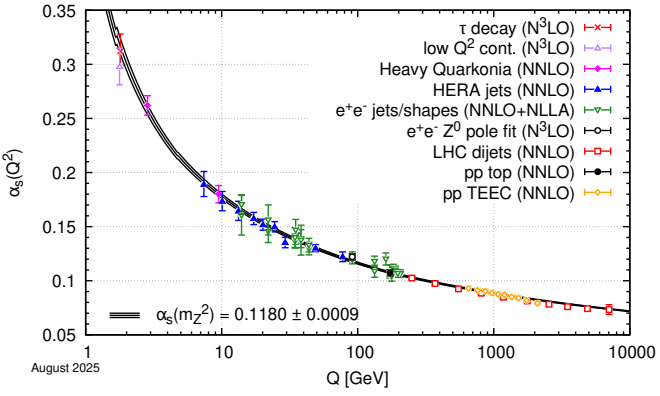

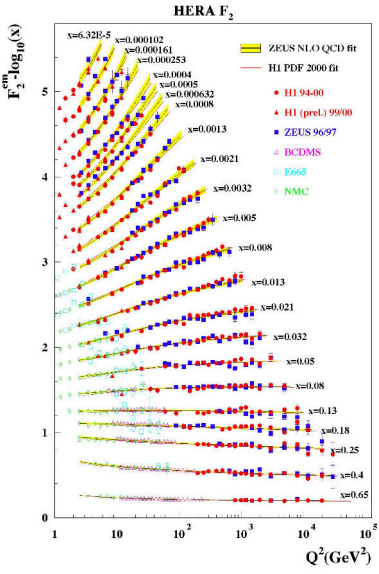

Above: QCD running coupling parameter $\alpha_s = g_3^2/(4\pi)$.

Right: structure function F_2 of the proton.

Scale dependence: perturbation theory.

Initial conditions: non-perturbative.

Why we are in the game: factorization of SM and QCD processes

Scale separation: $q \gtrsim \mu_F \gg \Lambda$

Short distance | Long distance

$$\underbrace{\sigma(q)}_{\text{cross section}} = \underbrace{C(q,\mu_F)}_{\text{coefficient function}} \otimes \underbrace{\langle O(\Lambda)\rangle(\mu_F)}_{\text{NP matrix element}} + O\left(\Lambda^2/q^2\right)$$

Coefficient function: **process-dependent**, perturbative.
Matrix element: **universal**, non-perturbative. Example: PDFs.

Cross sections do not depend on the **factorization scale μ_F.**

- For simplicity: **renormalization scale $\mu = \mu_F$.**
- Often also: **hard kinematic scale $q = \mu_F$.**

! Factorization does not always hold at arbitrary perturbative orders.

How to obtain NP matrix elements? Lattice QCD



Method is explained in Marvel's "Spiderman: Brand New Day". Christian Kummer, Monday, 16:00

Hadron structure map

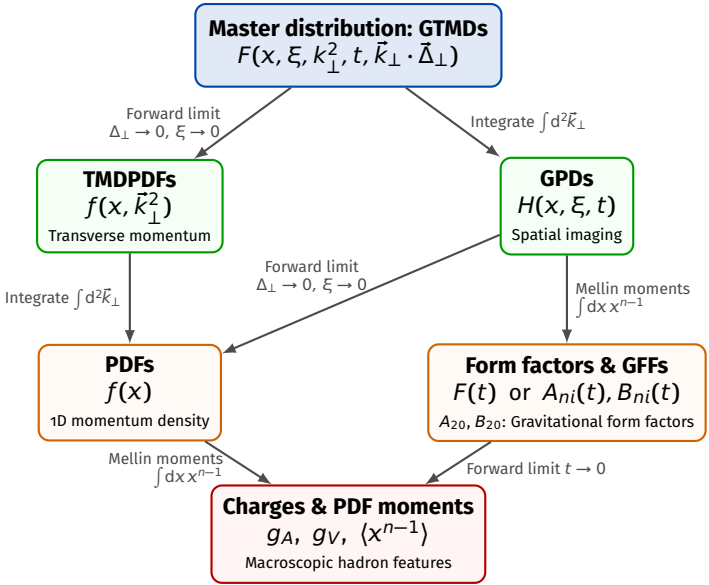

Kinematic definitions

- x: light cone "+" momentum fraction of parton. Forward limit: $x = x_B$.
- ξ: skewness: "+" momentum $P^+ \mapsto (1 - 2\xi)P^+ = P^+ + \Delta^+$.
- $\vec{k}_\perp$: Transverse parton momentum.
- $t = (\xi^2 M^2 - \vec{\Delta}_\perp^2)/(1 - \xi^2)$: squared hadron momentum transfer.
- Additional (logarithmic) dependence on the virtuality Q^2.

Hadron structure map

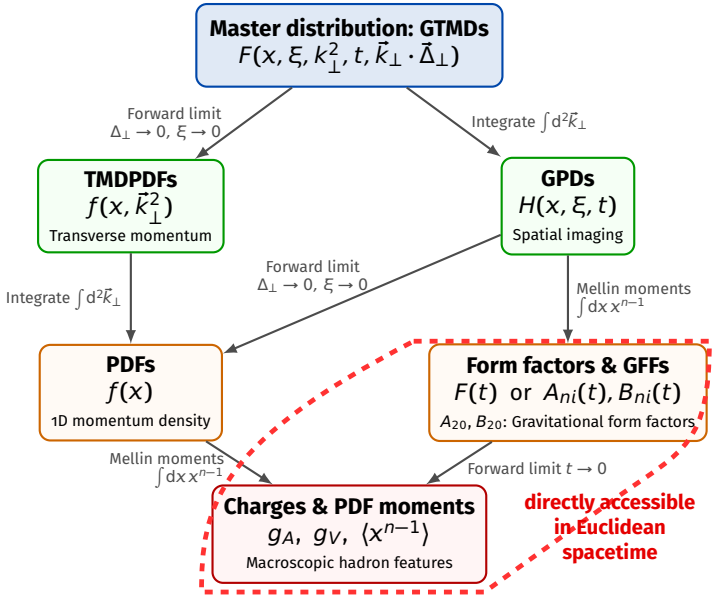

Kinematic definitions

- x: light cone "+" momentum fraction of parton. Forward limit: $x = x_B$.
- ξ: skewness: "+" momentum $P^+ \mapsto (1 - 2\xi)P^+ = P^+ + \Delta^+$.
- $\vec{k}_\perp$: Transverse parton momentum.
- $t = (\xi^2 M^2 - \vec{\Delta}_\perp^2)/(1 - \xi^2)$: squared hadron momentum transfer.
- Additional (logarithmic) dependence on the virtuality Q^2.

Other structure observables

- Transition form factors and GPDs.
  Christian Kummer, Monday, 16:00
  Gabriele Pierini, Monday, 18:00
  Poster Priajit Jana
  Poster Andreas Konstantinou
- What about resonances?
- Light cone distribution amplitudes.
- Higher twist contributions.
- Two-current observables, e.g., DPDs.

The major current nucleon structure experiments (+LHC)

EIC, JLab, MAMI

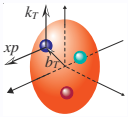

Map the 3-D structure of nucleons via GPDs and TMDs.

Complementary lattice calculations.

T2K, DUNE, NOνA

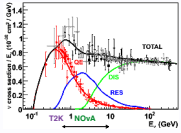

Axial form factor needed to predict $\sigma_{\nu N}$, $\sigma_{\nu A}$.

MESA (P2), JLab (MOLLER)

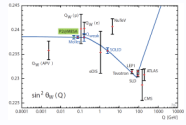

Parity violation expts. ($Q_W(p)$) need the $G^s_{E,M,A}(Q^2)$, $Z\gamma$ box diagrams.

MAGIX, PRad-II, ULQ2, MUSE, AMBER

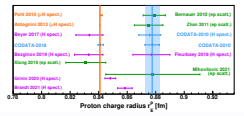

Proton charge/magnetic radius puzzle.

UCNA, Nab, PERC

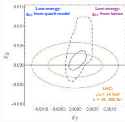

Precision β decay experiments.

$g_{S,T}$ needed to determine size of BSM contributions.

XENONnT, PandaX-4T, LUX-ZEPLIN

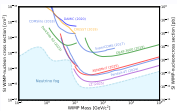

Direct dark matter detection: σ^q needed to predict the WIMP-nucleon cross-section.

Lattice QCD in more detail

Steps in the analysis:

Calculate correlation functions

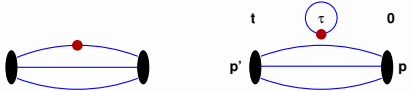

(Left) isovector ($u-d$) flavour combination.
(Right) isoscalar (u, d, s, c, g).

Fit

$$C^{\vec{p}',\vec{p},J}_{3pt,\Gamma_i}(t,\tau) \overset{t,\tau\longrightarrow\infty}{\longrightarrow} Ae^{-E_{\vec{p}'}(t-\tau)-E_{\vec{p}}\tau}\langle \boldsymbol{N}(\vec{\boldsymbol{p}}')|\boldsymbol{J}|\boldsymbol{N}(\vec{\boldsymbol{p}})\rangle$$

Matching from the lattice to a continuum scheme.

E.g. non-perturbative matching: lattice → RI′-(S)MOM scheme,
perturbative: RI′-(S)MOM → $\overline{\text{MS}}$.

Mixing between $q-g$ sectors, within the q sector (some actions).

See also Simone Bacchio, Wednesday, 12:15

Explore parameter space:

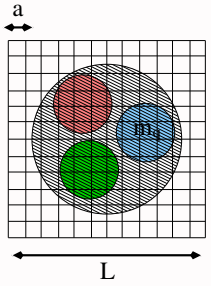

Finite volume, cut-off and quark mass dependence.

Cost of HMC: $\propto 1/(a^{\geq 6} M_\pi^{\approx 7.5})$

Perform extrapolation

$a \to 0$, $L \to \infty$, $M_\pi \to M_\pi^{\text{phys}}$

Challenges in the baryon sector

Meson sector: lattice provides (very) precise results for α_s, m_q, $q \in \{u/d, s, c, b\}$, form factors, see [FLAG 24, 2411.04268].

Statistical noise

Signal vs noise decays with $e^{-(E_N - 3M_\pi/2)t}$.

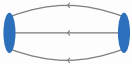

$$C_{2\text{pt}}(t) \overset{t\to\infty}{\longrightarrow} Ae^{-E_N t}$$

m_{eff} [GeV]

$$a^{-1} \ln \frac{C_{2pt}(t)}{C_{2pt}(t+a)}$$

$M_\pi = 340$ MeV

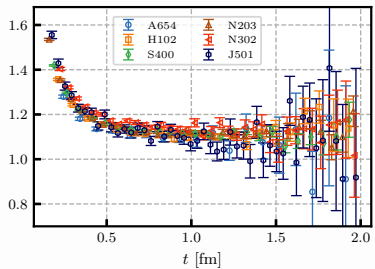

Excited state contributions

Dense spectrum of $N\pi$, $N\pi\pi$, ...states as $M_\pi \to M_\pi^{phys}$.

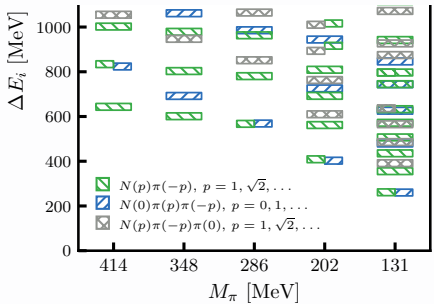

Parameterizing the quark-mass dependence: not clear how well ChPT describes the quark mass dependence in the range $M_\pi \sim (M_\pi^{phys} - 300$ MeV). → Need $M_\pi \approx M_\pi^{phys}$.

From matrix elements to hadron structure

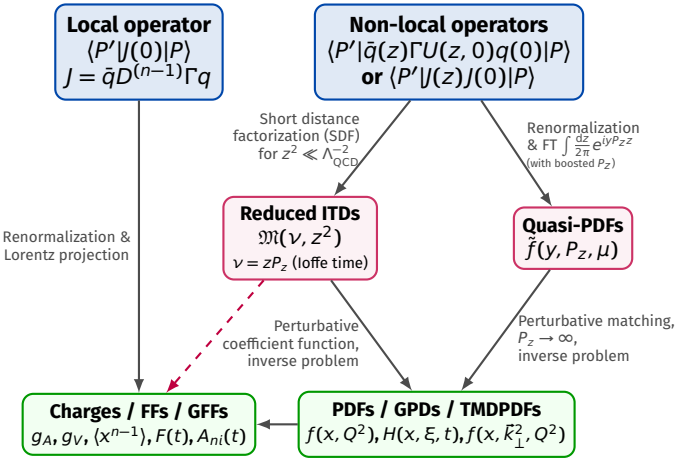

OPE of bilocal light-ray operator $O_\Gamma(z) = \bar{q}(z/2)\Gamma U(z/2, -z/2)q(-z/2)$:

$$O_\Gamma = \sum_{n\geq 0} \frac{1}{2^n n!} z^{\mu_1} \dots z^{\mu_n} \bar{q}(0)\Gamma \overleftrightarrow{D}_{\mu_1} \dots \overleftrightarrow{D}_{\mu_n} q(0)$$

Twist $\tau = d - s$: "spin" with respect to the conformal light front group $\mathrm{SL}(2, \mathbb{R})$.

d: Dimension of operator. s: Lorentz spin.

Leading twist: symmetrize and subtract traces.

Matrix elements $\langle P'|\bar{q}\cdots q|P\rangle$ then give **Mellin moments** of (fixed-twist) GPDs, i.e. GFFs.

Higher-twist contributions to scattering: usually suppressed by powers of Q.

Reduced ITDs (pseudo-PDFs) and quasi-PDFs
Inverse problem!
(same with PDFs from exp. cross-sections)

Higher-twist pollution:

$$\sim \Lambda^2 z^2 \text{ or } \frac{\Lambda^2}{x^2 P_z^2}, \frac{\Lambda^2}{(1-x)^2 P_z^2}.$$

Matching to continuum schemes

Matching (simplified picture)

For a given $\overline{\text{MS}}$ scheme matrix element

$$\langle O \rangle_{\overline{\text{MS}}}(\mu) = Z_O(\alpha(\mu), q) \cdot \langle O \rangle_{\text{lat}}(a, q) + \mathcal{O}(a^2 q^2)$$

Competing constraints

- **Continuum limit.** Only possible in the regime $q \ll a^{-1}$.
- **Perturbative matching.** Requires $\mu \gtrsim 2\,\text{GeV}$.
- **No large logs.** Requires $q \sim \mu$ to ensure a feasible perturbative expansion of Z_O.

Alternative:

Step scaling with $q \propto \mu = L^{-1}$.

Not always possible.

The window problem

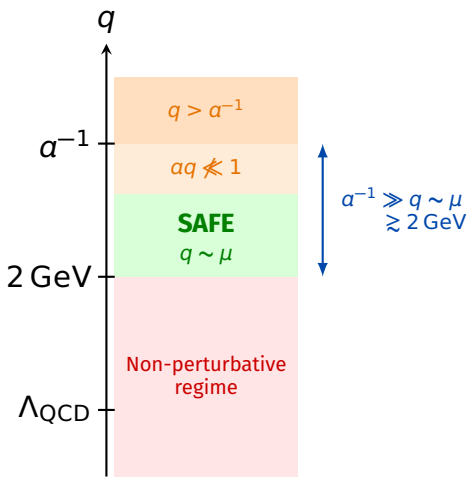

Electromagnetic form factors of the nucleon

$$\langle N(p')|J_\mu^{em}|N(p)\rangle = \bar{u}_N(p')\left(F_1^{p,n}(Q^2)\gamma_\mu + \frac{F_2^{p,n}(Q^2)}{2m_N}\sigma_{\mu\nu}Q^\nu\right)u_N(p)$$

$N \in \{p, n\}$, $J_\mu^{em} = \sum_q e_q V_\mu^q$, $V_\mu^q = \bar{q}\gamma_\mu q$ with $q \in \{u, d, s, \dots\}$.

Sachs FFs. $\quad G_E^{p,n}(Q^2) = F_1^{p,n}(Q^2) - \frac{Q^2}{4m_N^2}F_2^{p,n}(Q^2), \quad G_M^{p,n}(Q^2) = F_1^{p,n}(Q^2) + F_2^{p,n}(Q^2)$

Shape at low Q^2

$G(Q^2) = G(0)\left[1 - \frac{1}{6}\langle r^2\rangle Q^2 + \dots\right]$, $G_E^{\mathbf{p,n}}(0) = 1, 0$, $G_M^{p,n}(0) = \mu^{\mathbf{p,n}}$. Difficult to achieve low $Q^2 \neq 0$ (conventionally) → large L, $p_j = (2\pi n/L)$.

Extrapolation to reach $G_M(0) \to \mu$ and $\langle r_M^2\rangle$.

Some radii sensitive to M_π: $\langle r_{E,M}^2\rangle^{p-n}$ diverge as $M_\pi \to 0$.

Shape at high Q^2

Difficult due to signal to noise problem, excited states and cut-off effects.

(Most) lattice results within the range

$Q^2 \sim 0.04 - 1.00$ **GeV**^{2}**.**

Electromagnetic form factors of the proton and neutron

[Mainz 23, 2309.06590] full systematics included, [ETMC 25, 2507.20910] fit with the highest AIC weight shown.

$G_E^p(Q^2)$

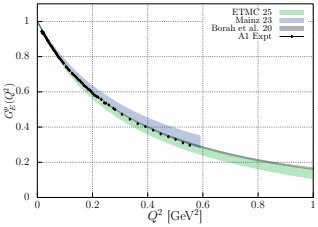

$G_E^n(Q^2)$

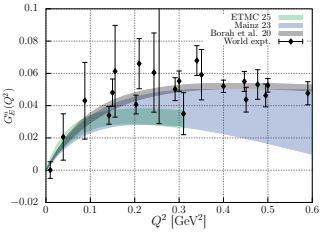

$G_M^p(Q^2)$

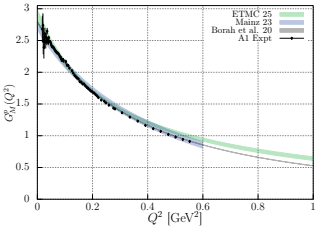

$G_M^n(Q^2)$

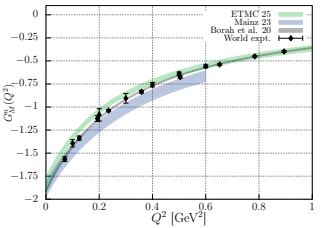

$G_{E,M}^{p,n}$ more difficult than $G_{E,M}^{p-n}$ due to noisy disconnected contributions.

[Borah et al., 2003.13640], [A1, 1307.6227], for world expt. see refs. in Borah et al..

Electromagnetic radii and magnetic moments

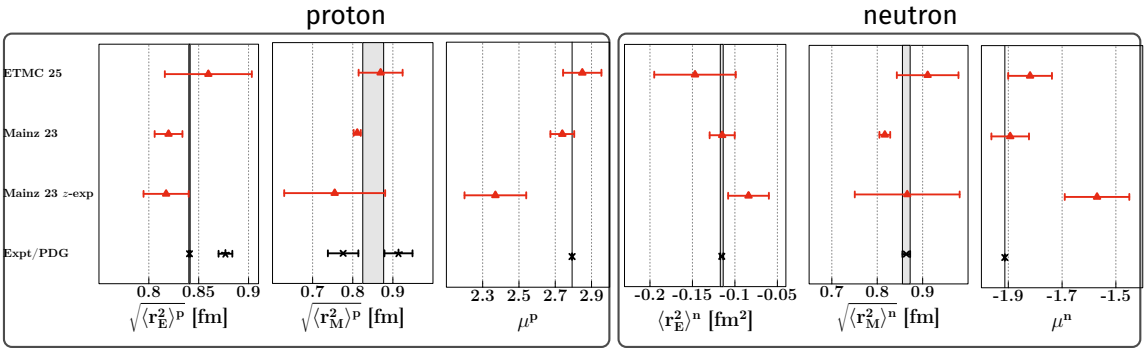

$\langle r_E^2\rangle^p$: CODATA 2022 (μH ✖), CODATA 2010 (ep+H spectroscopy ★).

$\langle r_M^2\rangle^p$: (ep) [Lee et al., 1505.01489] A1 (✖), world data excluding A1 (★), "puzzle": e.g., [Lin et al., 2412.12885].

Mainz 23: fit $G_{E,M}$ together using $O(q^3)$ covariant baryon ChPT [Bauer et al., 1209.3872].

Common LECs → reduced uncertainty on μ, $\langle r_M^2\rangle$ compared to independent z-expansion of $G_{E,M}$.

Axial form factors of the nucleon

- Long baseline ν-oscillation experiments produce ν_μ and $\bar{\nu}_\mu$ with a range of energies.
- E_ν reconstructed from detected decay products of interactions in the near and far detector.
  Range of interactions, nuclear effects, detector limitations, …
  → **Monte-Carlo simulation of the neutrino-nucleus (-nucleon) cross-section is needed.**

Neutrino-nucleon scattering cross-section

Quasi-elastic scattering (QE)

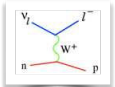

Resonance production (RES)

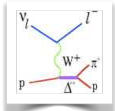

Deep Inelastic scattering (DIS)

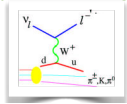

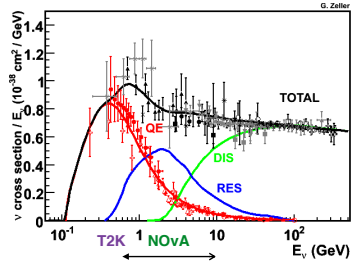

J.A. Formaggio, G. Zeller, Reviews of Modern Physics, 84 (2012)

14

QE: $\sigma_{\nu N}$ depends on

$$\langle p(p')|\bar{u}\gamma_\mu(1-\gamma_5)d|n(p)\rangle = \overline{u}_p(\text{EM FFs})u_n + \overline{u}_p\left[\gamma_\mu\gamma_5 \boldsymbol{G_A(Q^2)} + \frac{q^\mu}{2m_N}\gamma_5 \boldsymbol{\tilde{G}_P(Q^2)}\right]u_n$$

Contribution of $\boldsymbol{\tilde{G}_P(Q^2)}$ is suppressed.

Expt. information from scattering data:

$\bar{\nu}$-p and ν-D, expts. with nuclear targets and $\bar{\nu}$-H (within hydrocarbons), …

RES: first steps towards $N \rightarrow$ resonance transition matrix elements on the lattice.

Isovector axial form factor

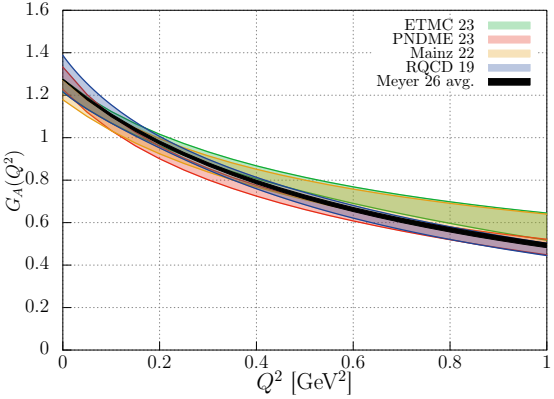

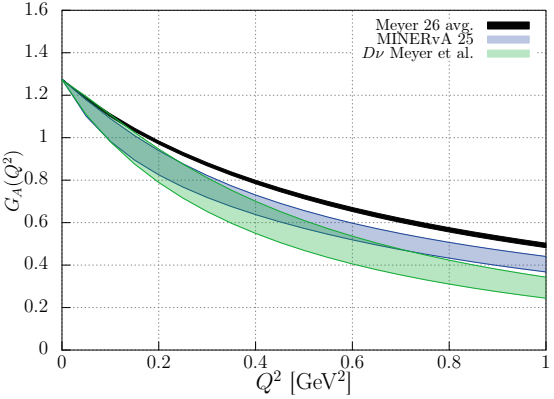

Lattice average: [Meyer 26, 2601.02676] ($G_A(0) = g_A$ fixed to experiment, also included [NME, 2103.05599]).

[ETMC 23, 2309.05774] [PNDME 23, 2305.11330] [Mainz 22, 2207.03440] [RQCD 19, 1911.13150]

[MINERvA 25, 2512.14097] ($\bar{\nu}$-H (in hydrocarbon molecules)) [$D\nu$ A Meyer et al, 1603.03048]. See also [O Tomalak et al, 2601.21155].

Isovector axial form factor: impact on the QE cross-section

[MINERvA, 2512.14097]

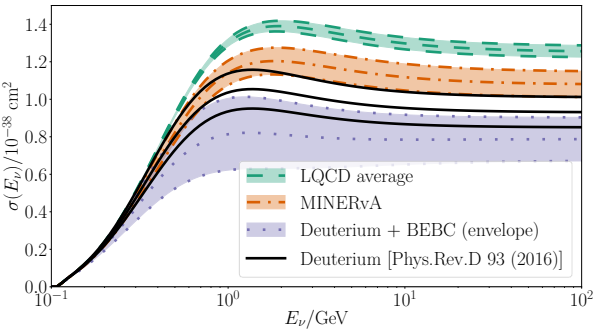

Slower fall-off of the lattice FF leads to a larger $\sigma_{\nu N}$.

[Meyer et al., 2201.01839] GENIE simulation of ν_μ-H2O charged-current QE event rates at near detector of T2K: 20% higher rate with a lattice G_A [CalLat, 2111.06333] compared to a dipole fit. $G_A(Q^2) = g_A/(1 + Q^2/M_A^2)$ with $M_A = 0.94$ GeV.

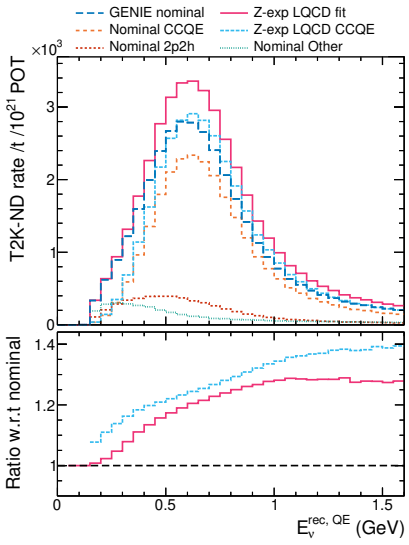

Isovector axial form factor: cross-checks

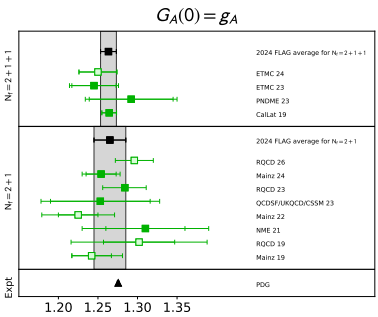

[RQCD, 1911.13150]

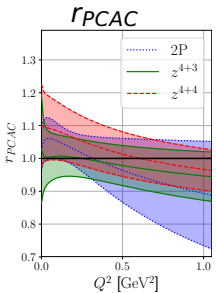

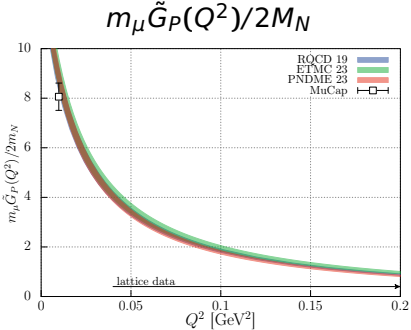

- PCAC relation reproduced in the continuum limit.

$$m_N G_A(Q^2)\mathbf{r_{PCAC}} = m_q G_P(Q^2) + \frac{Q^2}{4m_N}\tilde{G}_P(Q^2), \qquad \mathbf{r_{PCAC}} = 1 + \mathbf{O(a^2)},$$

where the **pseudoscalar form factor**: $\langle p(p')|\boldsymbol{P}|n(p)\rangle = \overline{u}_p i\gamma_5 \boldsymbol{G_P(Q^2)} u_n$.

- Induced form factor $\tilde{G}_P(Q^2)$ consistent with expt. at the muon capture point $Q^2 = 0.88\, m_\mu^2$.

Transition form factors involving resonances

For example, $N \to N\pi$ transition matrix elements: $N \to \Delta(1232)$, N^* resonances for vector and axial currents. (Pioneered by Cyprus.)

Straightforward if the resonance is stable ($m_\pi \nearrow$). $N \to \Delta$ and $N \to$ Roper previously studied.

$N \to$ resonance requires finite volume formalism for $N\pi \to N\pi$ ($2 \to 2$) scattering as well as $N \to N\pi$ ($1 + \mathcal{J} \to 2$). Meson $1 + \mathcal{J} \to 2$ transitions mostly studied so far, see, however, [Gao et al., 2310.01168,2502.12074] $\gamma^* N \to \pi N$.

First step: spectroscopy. Poster Ferenc Pittler

[Bulava et al., 2208.03867] $m_\pi = 200$ MeV

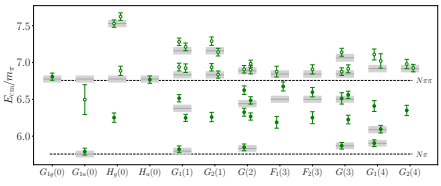

[ETMC, 2307.12846] $m_\pi^{\rm phys}$

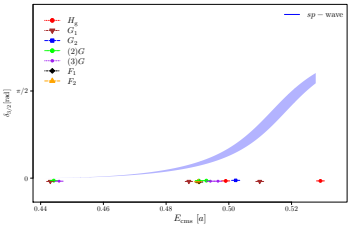

Computing $N \to N\pi$ matrix elements: [Barca et al., 2211.12278], [Barca, 2508.09006], [ETMC, 2408.03893], ...

Mellin moments of PDFs

Example of n-th moment of the unpolarised PDF:

$$\langle x^{n-1}(\mu)\rangle_{q^{(-)^n}} = \int_0^1 \mathrm{d}x\, x^{n-1}\left[q(x,\mu) + (-)^n \bar{q}(x,\mu)\right]$$

Notation: $q^- := q - \bar{q}\,(= q_v)$, $q^+ := q + \bar{q}\,(= q_v + 2\bar{q})$.

OPE connects the moments to **matrix elements of local operators**

$$\left\langle N(p)\left|\mathcal{O}^n_{\mu_1\ldots\mu_n}\right|N(p)\right\rangle \sim \langle x^{n-1}\rangle_{q^{(-)^n}}\left((p_{\mu_1}\cdots p_{\mu_n}) - \text{traces}\right)$$

$\mathcal{O}^n_{\mu_1\ldots\mu_n} = \bar{q}\gamma_{(\mu_1} i\overleftrightarrow{D}_{\mu_2}\ldots i\overleftrightarrow{D}_{\mu_n)}q$ where $(\mu_1\cdots)$: symmetrized, traceless.

$n = 1, 2, 3, \ldots$ operators are dimension 3, 4, 5, 6
and have 0, 1, 2, 3 . . . derivatives.

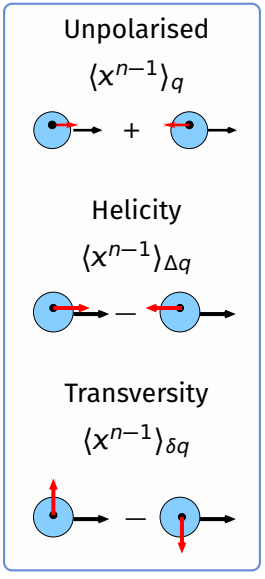

Mellin moments of PDFs

Information on the PDFs through moments.

- In principle, PDF can be reconstructed from moments. Large x requires high n.
- Lower moments can be used as constraints in phenomenological analyses.
- Determination of different flavour combinations is possible, also gluonic operators.
- There are no higher twist corrections. Matrix elements of higher twist operators computable.

However

- Signal to noise deteriorates as n increases.
- Renormalization: reduced symmetry on the lattice.
  If mixing with $n' = n - \ell$ is not prohibited by symmetry $\Rightarrow a^{-\ell}$ power divergencies.

Standard methods: fourth moment possible (e.g. in a boosted frame to avoid mixing).

New developments [Shindler, 2311.18704]: gradient flow approach gives improved signal and operator mixing like in the continuum. Poster Bolun Hu

First helicity moment $\langle 1 \rangle_{\Delta q^+}$, $\overline{\text{MS}}$, $\mu = 2$ GeV

Gauge invariant Ji spin decomposition of the nucleon

$$\frac{1}{2} = J_g + \sum_q J_{q^+} = \overbrace{J_g + \sum_q L_{q^+}}^{\text{dark spin}} + \overbrace{\sum_q \frac{1}{2}\Delta\Sigma_{q^+}}^{\text{quark spin}}, \qquad \Delta\Sigma_{q^+} = \langle 1 \rangle_{\Delta q^+}$$

L_q $J_{q,g}$

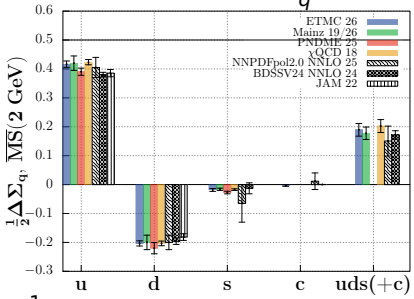

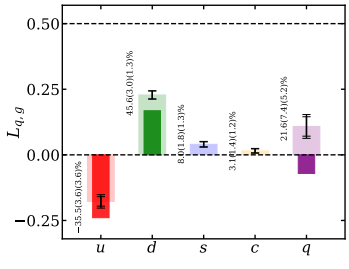

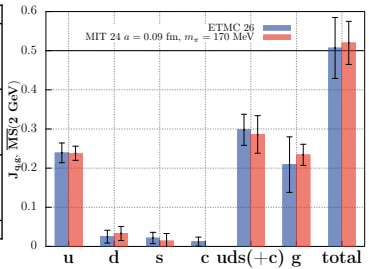

($\frac{1}{2}\Sigma_{q^+}$) [ETMC, 2607.21230], [Mainz 26, 2605.06559], [Mainz 19, 1911.01177], [PNDME 25, 2503.07100], [χQCD 18, 1806.08366], [NNPDFpol2.0NNLO, 2503.11814], [BDSSV24-NNLO, 2407.11635], [JAM 22, 2202.03372]. Poster Christof Iona, Yan Lo

($J_{q,g}$) [MIT 24, 2310.08484],[ETMC, 2607.21230] from moments of GPDs: generalized FFs $A_{20}^{q,g}(Q^2)$, $B_{20}^{q,g}(Q^2)$, $J_{q,g} = \frac{1}{2}[A_{20}^{q,g}(0) + B_{20}^{q,g}(0)]$, $L_{q^+} = J_{q^+} - \frac{1}{2}\Sigma_{q^+}$.

First transversity moment $\langle 1 \rangle_{\delta q^-}$, $\overline{\text{MS}}$, $\mu = 2$ GeV

[FLAG 24, 2411.04268]

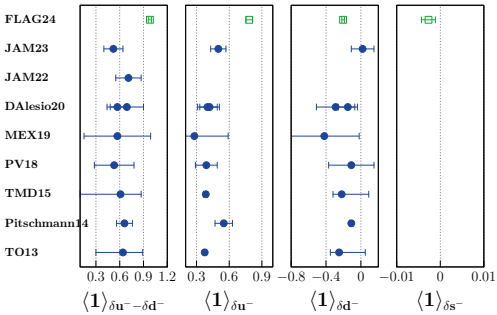

[JAM 23, 2306.12998]

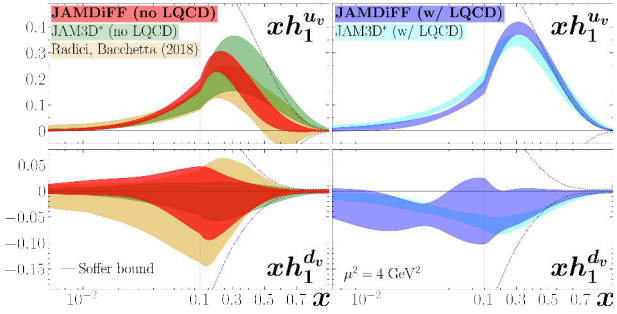

JAM 23: valence transversity PDFs $h_1^{u_v,d_v} \equiv h_1^{u,d} - h_1^{\bar{u},\bar{d}}$ from global analysis of dihadron production.

Constraints: [ETMC, 1909.00485] and [PNDME, 1808.07597] results for $\langle 1 \rangle_{\delta u^-}$ and $\langle 1 \rangle_{\delta d^-}$.

Soffer bound applied: (parton model) [Soffer, hep-ph/9409254] $|h_1^q(x)| \leq (q(x) + \Delta q(x))/2$.

FLAG 24: $\langle 1 \rangle_{\delta u^-, \delta d^-, \delta s^-}$ from [PNDME, 1808.07597]. Poster Christos Iona

Unpolarised second moment $\langle x \rangle_{q^+,g}$, $\overline{\text{MS}}$, $\mu = 2$ GeV

Quark and gluon momentum fractions: $\sum_q \langle x \rangle_{q^+} + \langle x \rangle_g = 1$.

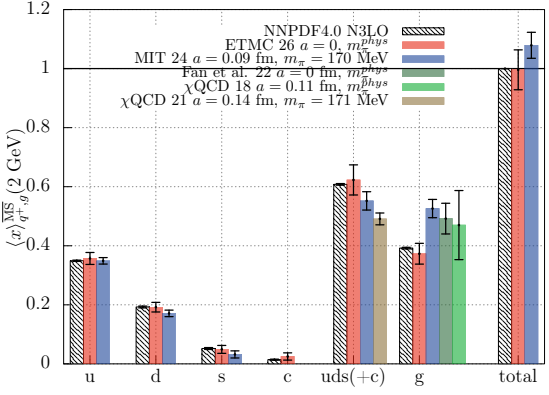

[NNPDF4.0N3LO, 2402.18635] (moments computed using [LHAPDF, 1412.7420]).

[ETMC, 2607.21230], [MIT 24, 2310.08484], [Fan et al. 22, 2208.00980], [χQCD 18, 1805.00531], [χQCD 21, 2111.09329]. Poster Yan Lo

Isovector unpolarised moments $\langle x^{n-1} \rangle$ up to $n = 4$, $\overline{\text{MS}}$, $\mu = 2$ GeV

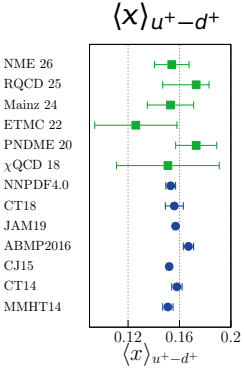

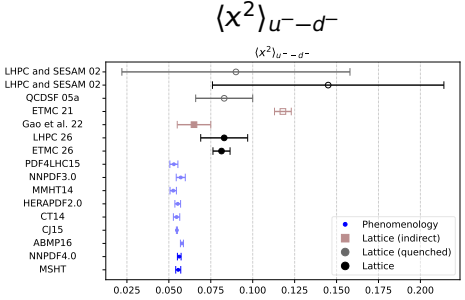

[LHPC, 2605.02808]

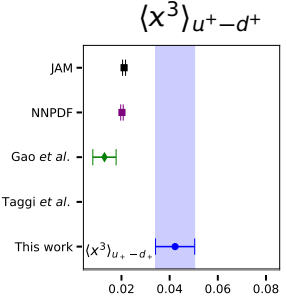

[ETMC, 2607.03458]

[LHPC, 2605.02808] (Fig. E. Taggi): $a \approx 0.116$ fm and $a \approx 0.093$ fm, $M_\pi \approx 135$ MeV.
Also $\langle x^2 \rangle_{\Delta u^+-\Delta d^+}$ and $\langle x^2 \rangle_{\delta u^--\delta d^-}$.

[ETMC, 2607.03458] $a \approx 0.08$ fm, $M_\pi \approx 139$ MeV. Also $u + d$, s and c (disconnected contributions neglected) and off-forward limit (moments of GPDs). Christian Kummer, Monday, 16:00

Higher moments with the gradient flow

Gradient flow: diffusion-like evolution in field space in auxilliary "flow" time t.

Smoothing over a range $\sqrt{8t}$.

Flowed theory: same symmetries as in the continuum.

No mixing with lower-dimensional lattice operators.

Improved signal to noise (no boost necessary).

Continuum limit

$$\langle x^{n-1}\rangle^{\text{flow}}(t) = \langle x^{n-1}\rangle^{\text{flow}}(t,a) + \underbrace{c_2\frac{a^2}{t} + \text{other } a^2 + \dots}_{\text{extrapolate } a\to 0}$$

Small flow time expansion

$$\langle x^{n-1}\rangle^{\overline{\text{MS}}}(\mu) = C_0^{(n)}(\alpha_s(\mu))\langle x^{n-1}\rangle^{\text{flow}}(t) + \underbrace{\sum_i c_{2i}^{(n)}\langle O_{n,2i}^{\text{flow}}\rangle\, t + \dots}_{\text{extrapolate } t\to 0}$$

Poster Bolun Hu

Figure: A. Shindler (OpenLat) Lattice 26 talk.

$\langle x^{n-1}\rangle_{u-d}$, $\mathbf{m_\pi = 300\ MeV}$, $a = 0.09 - 0.06$ fm.
Low statistics

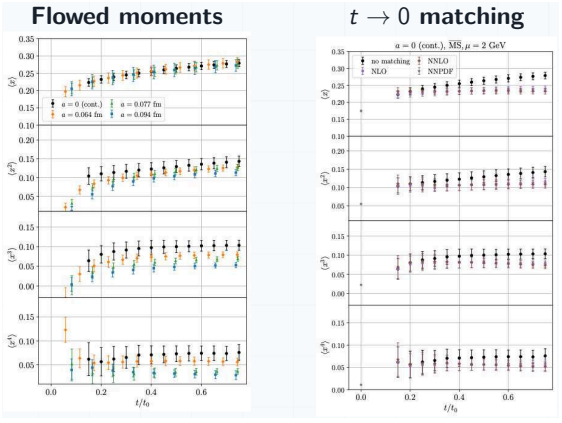

Moments of GPDs: generalised form factors, $\overline{\text{MS}}$, $\mu = 2$ GeV

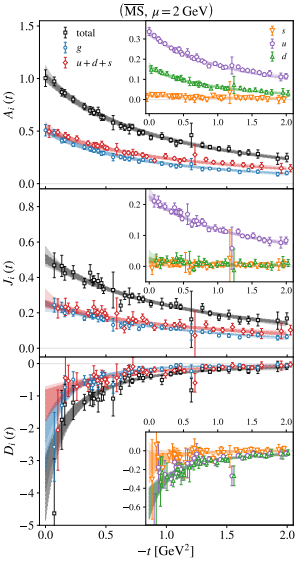

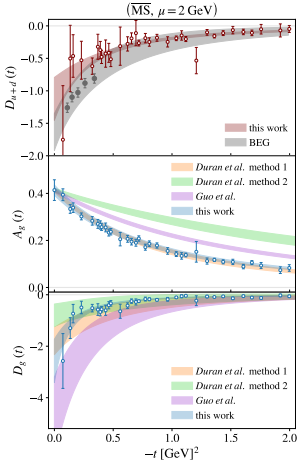

[MIT 23, 2310.08484]

$m_\pi = 170$ MeV, $a = 0.09$ fm.

Middle: $A_g(t)$ rescaled to give $A_g(0)$ of Duran and Guo.

[ETMC, 2607.20337]:

continuum limit, m_π^{phys}.

Matrix element of the traceless symmetric energy-momentum tensor

$\langle N(\vec{p}', s')|\hat{T}^{\mu\nu}|N(\vec{p}, s)\rangle$

depends on the GFFs:

$A_{q,g}(-t) = A_{20}^{q,g}(Q^2)$, $A(0) = \langle x \rangle$,

$J_{q,g}(t) = \frac{1}{2}[A_{20}^{q,g}(t) + B_{20}^{q,g}(t)]$,

and $D_{q,g}(-t) = C_{20}^{q,g}(Q^2)$.

2nd moments of unpolarised GPD:

$H \to A_{20}$ and C_{20}.

$E \to B_{20}$ and C_{20}.

Longitudinal force and energy density radii.

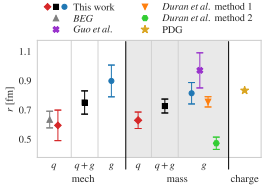

Summary of lattice hadron structure calculations

Importance

- **Essential tool:** Enables diverse experiments to achieve their full physics potential.
- **Meson precision:** Has become indispensable for flavour physics (not covered here).
- **Baryon frontier:** Achieving similar precision goals remains a key challenge.
- **Complementary input:** Straightforward flavour separation directly enhances global fits. Moments vs. x-dependence. Clean separation of leading twist.

Impact (examples)

- Impact on **helicity** and **transversity** PDFs!
- Steady progress on lesser-known **GPDs**, **TMDs**, and **gluon structure**.

Precision milestones

- Nucleon **charges and form factors** are approaching the **1% precision** threshold.
- Now that systematics are under control, the first two isovector PDF **Mellin moments** show agreement with global experimental fits.

Field vitality

- Higher Mellin moments are now accessible via **gradient flow** techniques.
- Wealth of interesting new coordinate-space data for **bilocal matrix elements**.
- Highly active landscape driving novel methods to improve calculational efficiency and to quantify systematic errors.